Experimental Observations on the Reaction of Unburned Pockets

Mark D. Frederick, Carson D. Slabaugh
Purdue University
West Lafayette, IN, USA

Joseph E. Shepherd
California Institute of Technology
Pasadena, CA, USA

1 Introduction

The purpose of this study is to experimentally investigate how and where diffusive transport manifests within a detonation and discuss its role in ignition and reaction of pockets of unburned gas behind detonation fronts. It is well established by analysis [1] and simulation [2] that diffusive transport of species cannot play a role in steady, one-dimensional models of detonation structure. However, this is not the case for unsteady [3] and multidimensional flows [4, 5]. This is particularly relevant [6] to highly unstable detonation waves [7] with apparently chaotic flow dynamics.

The universal instability of detonations results in a multi-dimensional, unsteady flow behind the front. A characteristic of these flows is the presence of strong velocity gradients due to the shear layers generated at the intersection of the transverse and leading shock fronts. These shear layers may transition to turbulence, they roll up into vortical structures, and are transported downstream of the front. These processes generate a cascade of length scales characterizing the concentration gradients [8] that enable diffusive transport to occur on time scales competitive with chemical reaction. In this way, diffusion emerges as a relevant process for any realistic description of highly unstable detonation waves.

Situations where diffusive transport may be relevant occur throughout a multi-dimensional detonation structure, both close-to and far-from the leading front. In the latter case, these pockets of slowly burning gas are referred to as "unreacted gas pockets" and have been discussed in previous studies [9, 10, 11]. As long as the pockets react completely before moving too far downstream from the leading shock front, the energy released is able to contribute to sustaining the detonation. When pockets appear close to the leading front, these regions often emerge immediately behind the the newly-formed, high-speed leading shock created after transverse wave collision. Vorticity is associated with the shear layers emerging from the triple points at the juncture of the leading shock and transverse waves [12, 13]. The dynamics of the shear layers in the unsteady flow behind the leading shock front results in high levels of turbulence capable of molecular mixing of reacted and partially or unreacted postshock gas. The combined action

Correspondence to: mfrederick@purdue.edu

of fluid motion and molecular diffusion have the potential to accelerate the reaction of the shocked but unreacted gas in the unburned pockets.

Two distinct manifestations of diffusive processes will be described and analyzed. The first involves the appearance of unreacted gas pockets that are made visible through the use of OH Planar Laser Induced Fluoresce (PLIF) imaging. The second involves a delayed explosion that occurs directly behind a newly formed high-speed shock. The reaction and mixing time-scales of these phenomena will be discussed in the context of the overall detonation wave structure.

2 Experiment Description

Experiments were carried out in the *Narrow Channel Facility* (NCF), a rectangular channel (152.4 x 17.78 mm) developed at the Explosion Dynamics Laboratory at Caltech [14] and currently operated at Zucrow Laboratories. Detonations of premixed gases are directly initiated with an acetylene-oxygen driver to create a nominally two-dimensional detonation wave. Detailed information regarding the design, operation, and previous findings with this facility are available in earlier publications [7, 14, 15, 16].

Schlieren imaging was performed in a lens-type configuration with a pulsed light-emitting diode (LED) light-source. 128 images were record at a rate of 5 MHz on a Shimadzu HPV-X2 high-speed camera. The detector size was 400 x 250 pixels and had a field of view of 54.8 x 34.2 mm, yielding a spatial resolution of 137 $\mu\mathrm{m/px}$. A second Shimadzu HPV-X2 simultaneously recorded the broadband chemiluminescence emission of the detonation. This camera was placed above the schlieren beam path and angled downwards at nine degrees to achieve a coincident field of view with the schlieren.

The OH PLIF system consisted of a flash-lamp pumped, Nd:YAG burst-mode laser (BML) (Spectral Energies QuasiModo) and an optical parametric oscillator (OPO). The BML produced a short burst of high-energy pulses at 300 kHz and with a 10 ns pulse width. The duration of the pulse train was limited to what was needed to resolve the wave passage through the field of view. The frequency-doubled (532 nm) and -tripled (355 nm) output of the BML provided 40 mJ/pulse and 80 mJ/pulse, respectively. The OPO produced about 14 mJ/pulse at the signal wavelength and was then mixed with the 532 nm output of the BML in a beta-Barium borate (BBO) crystal cut at 43° (sum-frequency-generation) to produce a ≈284 nm beam with an energy of 0.9 mJ/pulse. Further details of the PLIF system can be found in Frederick *et al.* [17].

3 Results and discussion

Two cases of unique mixture composition will be examined in this work. Case (A) is a mixture of stoichiometric methane and oxygen diluted with 33% nitrogen and case (B) is stoichiometric hydrogen and oxygen diluted with 57% nitrogen. The initial conditions for each case are listed in Table 1 along with computed detonation parameters. High-frequency pressure transducers distributed axially along the channel were used to measure the wave speed of each case before the wave reached the window section. Case (A) was traveling at an average speed of 95% of the Chapman-Jouguet speed ($\mathrm{U_{CJ}}$) and case (B) was travel at 90% of $\mathrm{U_{CJ}}$. As has been extensively documented in our previous studied, significant fluctuations in the leading front speed occur about the average values.

A selected number of schlieren images for case (A) are shown in Figure 1. The sequence begins just after transverse wave collision (frame a) and growing out of the collision is a new high-speed shock (i). Transverse waves (ii) and (iii) move laterally upwards and downwards, respectively. Behind the high-speed leading shock and between the transverse waves is a distinct zone (iv), which contains gases that react through a unique path compared to the surrounding fluid. This zone will be one of the main

Table 1: Calculated detonation parameters. P_0 is the initial pressure, T_0 is the initial temperature, τ_I is the induction time, and τ_E is the exothermic time. All parameters are calculated using the Zel'dovich-von Neumann-Döring (ZND) model using the Shock and Detonation Toolbox [18] with the GRI3.0 reaction mechanism [19].

Case	Mixture	P_0 [kPa]	T_0 [K]	U_{CJ} [m/s]	τ_I [μs]	τ_E [μs]
A	CH_4-$2O_2$-$1.5N_2$	21.1	300	2106	12.8	0.23
B	$2H_2$-O_2-$3.9N_2$	29	300	1929	1.9	0.44

topics of discussion in this work. The accompanying chemiluminescence field for this case (A) is shown in Figure 2. These frames illustrate the reaction progress occurring within zone (iv) and were selected to have a smaller time-interval to allow for the progression to be observed. The key features are called out using the same labels as Fig. 1.

In the schlieren images, zone (iv) can been seen expanding from frames (b) - (g) of Fig. 1. As it expands, there are intensity fluctuations in the chemiluminescence field (see frames (a) - (d) of Fig. 2). These fluctuations are indicative of reaction enhanced by diffusive transport occurring within the zone and are best observed by watching the video for this case. The turbulent processes that engender the mixing needed to support such a reaction are likely provided by vortical structures that were produced when the transverse waves collided [20, 21]. These are often described as "jetting structures" and were first experimentally observed by Subbotin [12].

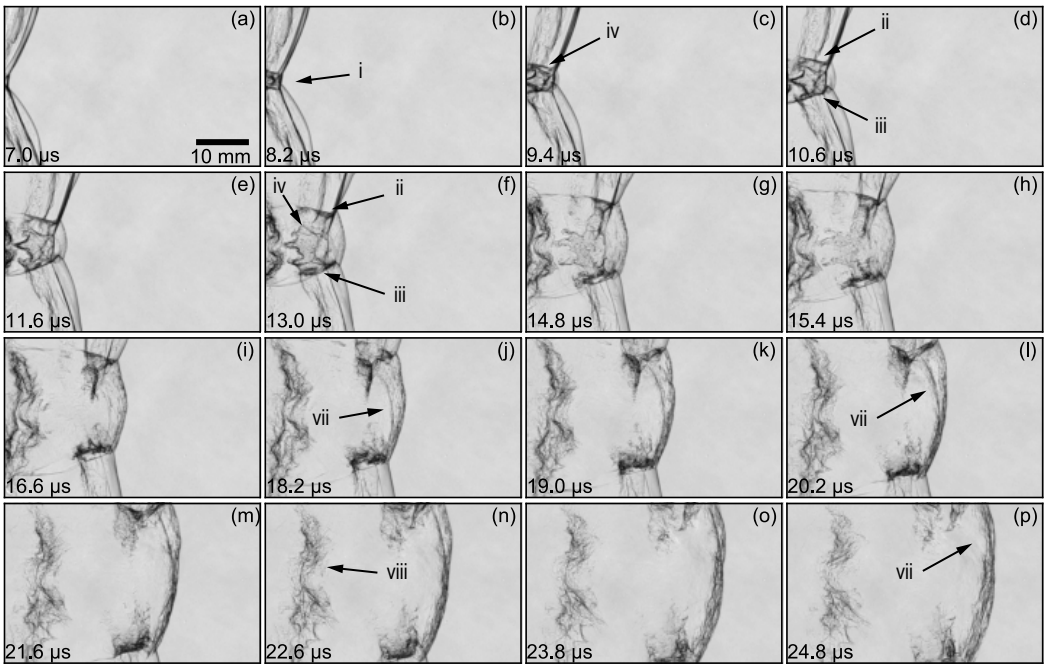

Figure 1: Selected schlieren images of case (A). Key features are described in the text.

Frame (h) of Fig. 1 and frame (e) of Fig. 2 show the same instant in time and capture the explosion of the zone (iv). In the schlieren image, the previously distinct boundary fades and, more obviously, in the chemiluminescence a high-intensity region (v) appears. As time progresses, a circular wave emanating from the site of explosion expands and is particularly noticeable at later times in the chemiluminescence images (see Fig. 2k). The clear appearance of this explosion, which is secondary to the explosion immediately following transverse wave collision, is unique among the hundreds of cases the authors have analyzed. Further analysis will be performed to model the conditions and reaction time-scales

within the zone (iv) to better understand the onset of the secondary explosion. A constant pressure, well-stirred reactor model will be used to understand how the reaction-rate within the zone would be accelerated through vorticity induced mixing of hot products with cooler, unreacted gas. A similar analysis was performed by Qi and Shepherd [22] to model ignition in under-expanded jets.

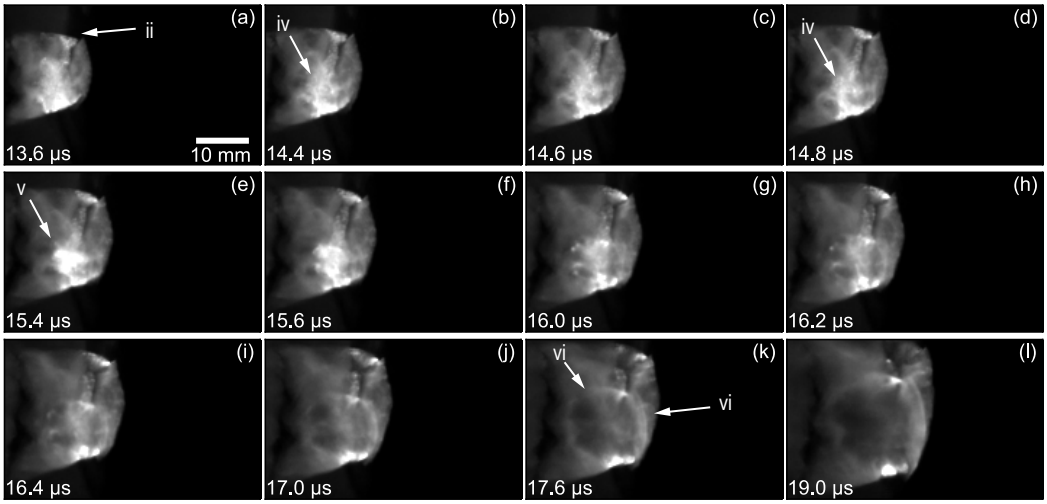

Figure 2: Select chemiluminescence images of case (A). Labels correspond to those in Fig. 1.

The impact that the explosion has on the wave system is measured by creating a velocity map [16] from the schlieren images and extracting the shock-front speed through the center of this cell. The velocity map and velocity trace are shown in Figure 3. Upon transverse wave collision, the wave speed rapidly increases to $\approx 1.45 U_{CJ}$. After this the wave speed then decreases but does not drop to sub-U_{CJ} speeds as has been measured in other unstable cases [16]. The wave speed remains greater than U_{CJ} for the duration of the recording. It is possible that the secondary explosion acts to "reinforce" the leading front and maintain a wave speed greater than U_{CJ}. Support for this hypothesis is provided in the schlieren images. As a result of the secondary explosion, feature (vii) accelerates toward the leading-front and becomes coincident in frame Fig. 1(p).

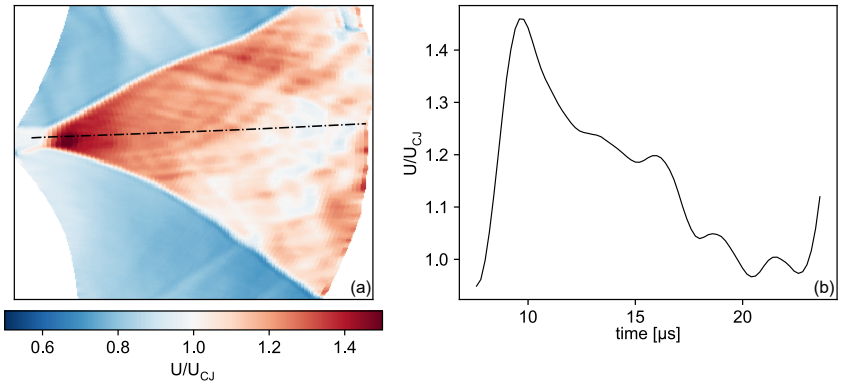

Figure 3: Velocity map of case (A) with black dotted extraction line, (a). The velocity trace taken along the extraction line, (b).

The second manifestation of diffusive transport in case (A) is within the unreacted gas pocket, which forms after the unreacted gases that collect in the shear layers detach from the leading front following transverse wave collision. This pocket is identified as feature (viii) in Fig. 1(n). The lack of reactivity within this gas pocket is made apparent by examining the OH PLIF image in Figure 4, in which the

region of (viii) is dark while being surrounded by fluorescence. Burnout of this pocket is not clearly identifiable for case (A), but is more definitive in the PLIF images of case (B) shown in Figure 5.

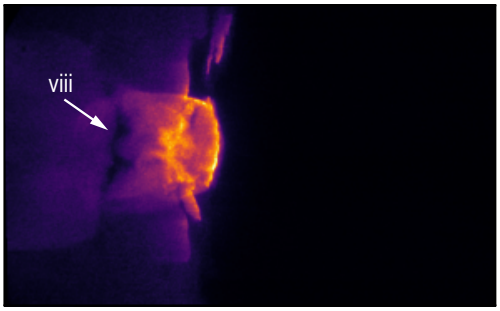

Figure 4: OH PLIF image from case (A).

Case (B) has been qualitatively discussed in a previous publication by Frederick *et al.* [17]. It shows an unreacted gas pocket, feature (vi) in frame 5(b), forming and later burning in frames (g) - (i). The burning of these pockets is likely caused by the diffusive mixing of the surrounding products with the unreacted gases inside the pocket. Further analysis will be performed to model the burnout time of these pockets in order to understand how their consumption may influence the overall propagation of the wave system.

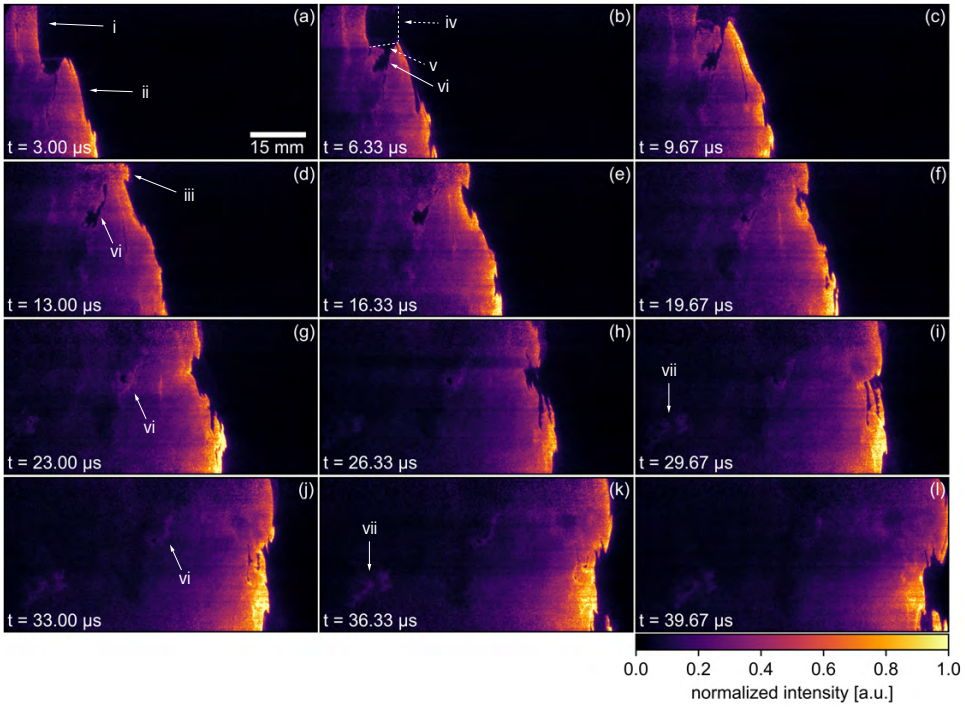

Figure 5: Time-series of OH PLIF images for case (B). The labeled features are: (i): decoupled reaction zone, (ii): high-speed shock, (iii): newly formed high-speed shock, (iv): low-speed shock, (v): transverse wave, (vi): unreacted/reacting gas pocket, (vii): second reacting gas pocket.

Acknowledgments

This work was supported by U.S. Air Force Office of Scientific Research grant FA9550-21-1-0013 (PO: Dr. Chiping Li)

References

[1] J. Clarke, "Fast flames, waves and detonation," *Progress in Energy and Combustion Science*, vol. 15, pp. 241–271, Jan. 1989.

[2] S. Singh, D. Lieberman, and J. E. Shepherd, "Combustion behind shock waves." Paper 03F-29 Western States Section/Combustion Institute, October 2003.

[3] C. M. Romick, T. D. Aslam, and J. M. Powers, "Verified and validated calculation of unsteady dynamics of viscous hydrogen–air detonations," *Journal of Fluid Mechanics*, vol. 769, pp. 154–181, Apr. 2015.

[4] J. L. Ziegler, R. Deiterding, J. E. Shepherd, and D. I. Pullin, "An adaptive high-order hybrid scheme for compressive, viscous flows with detailed chemistry," *Journal of Computational Physics*, vol. 230, pp. 7598–7630, 2011.

[5] J. L. Ziegler, *Simulations of Compressible, Diffusive, Reactive Flows with Detailed Chemistry Using a High-Order Hybrid WENO-CD Scheme*. PhD thesis, California Institute of Technology, 2011.

[6] M. Arienti and J. Shepherd, "The role of diffusion in irregular detonations." The 4th Joint Meeting of the US Sections of the Combustion Institute, Philadelphia, PA, March 20-23, 2005.

[7] J. Austin, F. Pintgen, and J. Shepherd, "Reaction zones in highly unstable detonations," *Proc. Combust. Inst.*, vol. 30, no. 2, pp. 1849–1857, 2005.

[8] P. E. Dimotakis, "Turbulent Mixing," *Ann. Rev. Fluid Mech.*, vol. 37, pp. 329–356, 2004.

[9] D. H. Edwards, A. T. Jones, and D. E. Phillips, "The location of the Chapman-Jouguet surface in a multiheaded detonation wave," *Journal of Physics D: Applied Physics*, vol. 9, no. 9, pp. 1331–1342, 1976.

[10] C. B. Kiyanda and A. J. Higgins, "Photographic investigation into the mechanism of combustion in irregular detonation waves," *Shock Waves*, vol. 23, pp. 115–130, 2013.

[11] M. I. Radulescu, G. J. Sharpe, C. K. Law, and J. H. S. Lee, "The hydrodynamic structure of unstable cellular detonations," *Journal of Fluid Mechanics*, vol. 580, p. 31–81, 2007.

[12] V. Subbotin, "Collision of transverse detonation waves in gases," *Combust. Explos. Shock Waves*, vol. 11, no. 3, pp. 411–414, 1975.

[13] G. Ben-Dor, *Shock Wave Reflection Phenomena*. Berlin: Springer, 2 ed., 2007.

[14] J. M. Austin, *The role of instability in gaseous detonation*. PhD thesis, California Institute of Technology, 2003.

[15] J. Austin and J. Shepherd, "Detonations in hydrocarbon fuel blends," *Combust. Flame*, vol. 132, no. 1, pp. 73–90, 2003.

[16] M. D. Frederick, R. M. Gejji, J. E. Shepherd, and C. D. Slabaugh, "Reactive processes following transverse wave interaction," *Proceedings of the Combustion Institute*, vol. 40, 1 2024.

[17] M. D. Frederick, R. M. Strelau, R. M. Gejji, J. E. Shepherd, and C. D. Slabaugh, "300 kHz OH PLIF of detonation structure," in *AIAA SCITECH 2024 Forum*, pp. 2024–1031, 2024.

[18] J.E. Shepherd, "Shock and Detonation Toolbox," 2021. https://shepherd.caltech.edu/EDL/SDT/.

[19] G. P. Smith, D. M. Golden, M. Frenklach, M. W. Moriarty, B. Eiteneer, M. Goldenberg, C. T. Bowman, R. K. Hanson, S. Song, W. C. Gardiner, V. V. Lissianski, and Z. Qin, "GRI-Mech," July 1999.

[20] S. S. Lau-Chapdelaine, Q. Xiao, and M. I. Radulescu, "Viscous jetting and Mach stem bifurcation in shock reflections: Experiments and simulations," *J. Fluid Mech.*, vol. 908, no. 1986, 2020.

[21] A. Sow, S. M. Lau-Chapdelaine, and M. I. Radulescu, "The effect of the polytropic index γ on the structure of gaseous detonations," *Proceedings of the Institute*, vol. 38, no. 3, 2021.

[22] Y. Qi and J. E. Shepherd, "Ignition of hexane-air mixtures by highly under-expanded hot jets," *Proceedings of the Combustion Institute*, vol. 39, pp. 2979–2990, 1 2023.